PAPER • **OPEN ACCESS**

The problem of quality assessing for the methods of coherence maps calculation in InSAR remote sensing of the Earth data processing

To cite this article: A V Sosnovsky *et al* 2019 *J. Phys.: Conf. Ser.* **1368** 032023

IOP Publishing
1368 (2019) 032023 doi:10.1088/1742-6596/1368/3/032023

The problem of quality assessing for the methods of coherence maps calculation in InSAR remote sensing of the Earth data processing

A V Sosnovsky[1], V G Kobernichenko[1] and N S Vinogradova[1]

[1]Ural Federal University, Mira st., 19, Ekaterinburg, Russia, 620002

e-mail: sav83@e1.ru

Abstract. Interferometric coherence is an important indicator of the quality of interferograms obtained by synthetic aperture interferometric radars (InSAR), because the areas with low coherence are not suitable for interferometric data processing. The coherence value is used as a parameter for adaptive phase noise suppression algorithms. It can also be used for surface classification tasks. The paper investigates the problem of the coherence estimate reducing under the influence of the topographic phase slope and considers ways to reduce the impact of the slope on the estimate value. The paper presents a comparative efficiency analysis of four methods for coherence maps calculation used for the phase noise suppression on the interferograms by a spectral adaptive filter in interferometric data processing for the Earth's remote sensing space radar ALOS PALSAR

1. Introduction

The method of space radar interferometry, which essence is the joint processing of phase fields obtained by imaging the same area simultaneously with two antenna systems or by one antenna on two orbits, combines the high accuracy of the phase method of measuring range with high resolution of space synthesized aperture radars (SAR) [1-5]. This technique makes it possible to obtain digital elevation models (DEM) and displacement maps from multiple radar observations.

One of the general problems of interferometric data processing is the decorrelation of radar echoes, or the loss of reflected electromagnetic waves coherence, which is caused by the difference in the imaging angle (geometric decorrelation), changes in the surface or propagation medium within the imaging interval (temporary decorrelation), and the radio waves volume scattering for some types of surfaces. The decorrelation degree varies for different types of surfaces from the almost complete coherence (small vegetation, urban areas using high and ultra-high-resolution SAR) to complete decorrelation (water surfaces, forest vegetation using centimeter and higher-frequency waves in SAR). Thus, the accuracy of the result (DEM or elevation displacement map) will depend significantly on the type of surface and imaging conditions.

To estimate the signal decorrelation level, coherence maps are used [1], which represent a field of correlation coefficients between two or more radar images on the same territory. Using the accepted system of formalization, coherence map elements can take values in the range from 0 to 1 with the zero-value corresponding to the complete terrain decorrelation, and the value of 1, on the contrary, corresponding to the absolute correlation of the scenes fragments. The coherence map characterizes the deviation degree of the absolute phase from the true value, and this deviation can be caused by both changes of the Earth's surface or the dielectric properties of the objects located on it. Figure 1 shows two coherence maps for the same area generated for ALOS PALSAR data, the first of the images being obtained from SAR pairs at two-week intervals and the second from 13-month intervals.

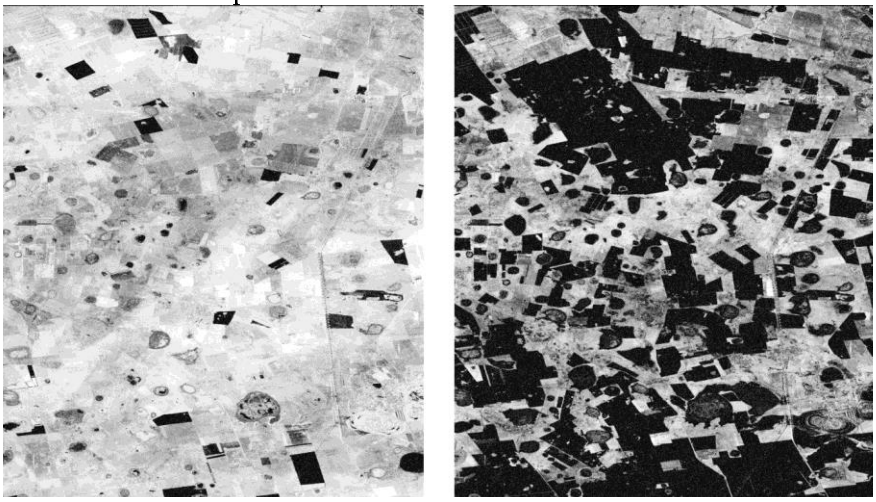

a) b)

Figure 1. Example of coherence maps obtained for different time periods: a) two weeks, b) thirteen months.

Areas with different coherence corresponding to different types of underlying surface are clearly visible in the images. It should also be noted that for the coherence map in figure 1a the light shades are dominated, which indicates a high correlation between the two images of the SAR pair, while in figure 1b the image is predominantly dark. In this case, the correlation is low due to natural changes on the earth's surface that occurred over a period of 13 months. Coherence maps are widely used as independent products in various radar tasks, for example, assessing the quality of the results of interferometric processing [6,7], segmentation of radar images [8-10], as well as intermediate data during interferometric processing.

The classical method of constructing maps is based on multiplying the first (reference, or master) image of an interferometric pair by the second (auxiliary, or slave), complex-conjugate to itself [1,8]:

$$\hat{\gamma}_0 = \frac{\left|\sum \dot{z}_1(i,j)\cdot \overline{z}_2(i,j)\right|}{\sqrt{\sum \left|z_1(i,j)\right|^2 \cdot \sum \left|z_2(i,j)\right|^2}} \tag{1}$$

where $\dot{z}_1, \dot{z}_2$ are the radar images of the reference and auxiliary signals, respectively, the summation is carried out in the local evaluation window size M×N (azimuth and range, respectively). However, when (1) is used in the task of estimating of the complex radar images coherence, a problem arises, which is expressed in the influence of the regular (topographic) component of the phase on the value of the estimate itself. The elimination of such influence requires the use of other estimates or modifications of the estimates and, accordingly, the study of the effectiveness of such modifications. To compare the effectiveness of an approach to evaluation, one can rely on the success of the estimate for a particular application. In this paper, we investigate the efficiency of using different coherence estimates in the problem of phase noise filtration in interferometric processing.

2. Methods of coherence maps calculation

The estimate (1) represents a formula for calculating the correlation coefficient of two complex random variables. However, complex radar images are not the sets of random variables, but two-dimensional complex random processes, which are, in general case, non-stationary, and in the presence of the differential phase slope (phase ramp) the estimate according to the formula (1) acquires an additional bias associated with the slope value. This effect in the one-dimensional case can be demonstrated using the model of the differential phase of two signals $\Delta\varphi$ correlated with a constant coefficient close to one. If the difference phase is constant (figure 2a), the correlation coefficient module estimate (1) will not shift ($\hat{\gamma}_0 = 0.9$). If the difference phase has a slope (figures 2b, 2c), then the estimate value $\hat{\gamma}_0$ begins to move downwards, and it depends more on the angle of the phase slope, but not on the ratio of the topographic and noise components of the interferogram ($\hat{\gamma}_0 = 0.5$ and $\hat{\gamma}_0 = 0.2$ accordingly).

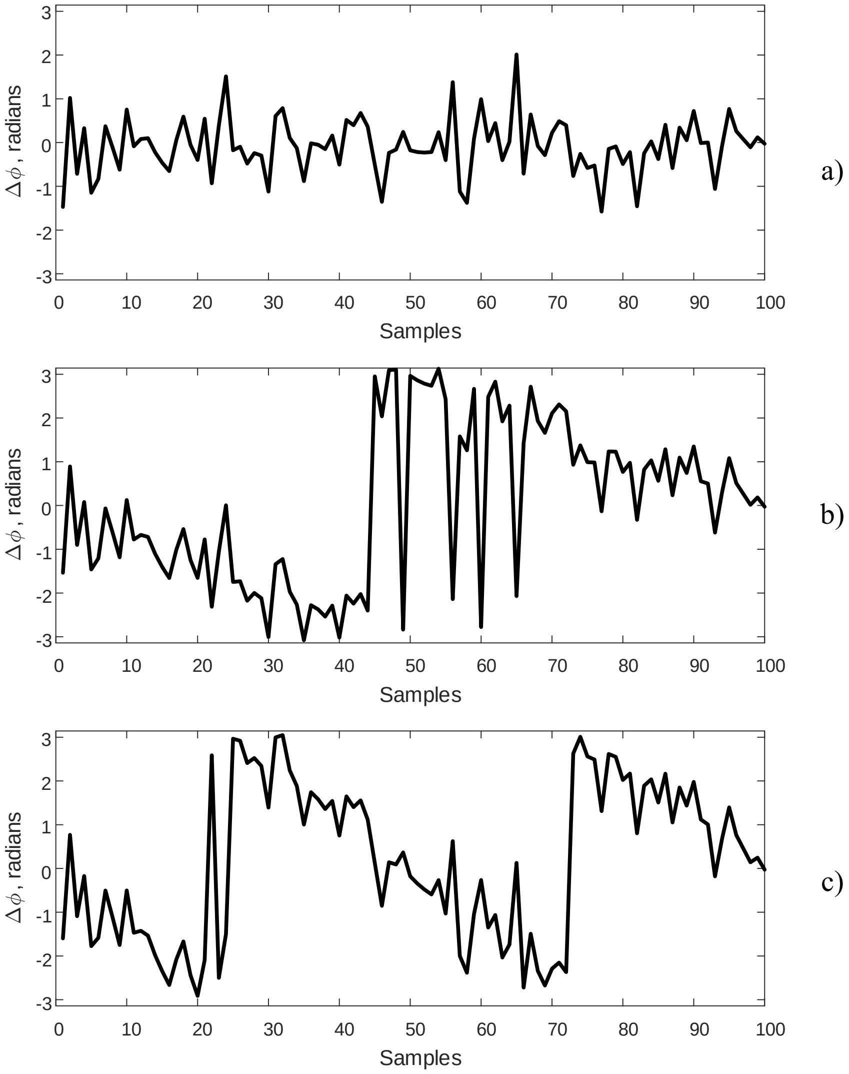

Figure 2. The differential phase of two complex Gaussian random processes at a constant level of phase noise and different phase slope angle: a) no slope; b) 2 rad per 100 samples; c) 4π rad per 100 samples.

The value of the estimator bias depends on both the rate of phase change (ramp angle) and the sample window size, *i.e.* the size of the coherence estimation window. Let us estimate this bias under different conditions.

1. Let us simulate pairs of random processes with given correlation coefficients between the corresponding counts (0.95, 0.7 and 0.1). The size of the estimation window will be 11×11. Next, changing the angle of the trend in the range from 0^{o} to 360^{o} in increments of 1^{o}, the estimation the coherence by the formula (1) is made. The results are shown in figure 3a, which shows that for the angles of about 30° the estimate downgrades to the value of about 0.25 regardless the value of the initial correlation coefficient, which corresponds to the shift of the correlation coefficient estimate for a pair of completely uncorrelated samples of the size equal to the size of the evaluation window.

2. For the same processes, we use a fixed correlation coefficient (0.7) and different sample sizes: 3×3, 7×7 and 11×11, respectively. Changing, as before, the ramp angle and evaluating the coherence,

we obtain the results presented in the graphs of figure 3b, from which it is clear that for increasing the evaluation window, the bias is noticeably increased, too. The bias manifests itself at noticeably smaller angles (units of degrees), and its value becomes almost equal to the value of the estimate itself.

Thus, for the changing forms of relief, the estimation of the coherence of the interferogram calculated by the formula (1) does not make it possible to estimate the ratio between the topographic and fluctuation components of the differential phase.

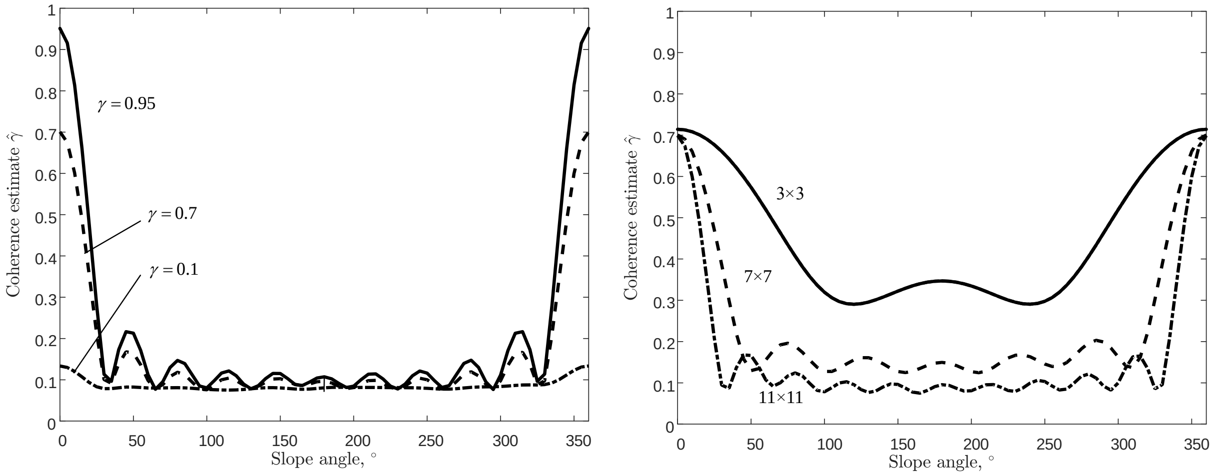

a) b)

Figure 3. Estimation bias under the slope (ramp) influence: a) for three different coherence (correlation) coefficients; b) for three different estimation window sizes.

The problem of the coherence estimation bias under the influence of the differential phase slope and the methods of reducing this influence were considered in [11,12], and two main ways were distinguished. The first implies the construction of estimates using the information about the images' amplitude or intensity, only, and, the second, is the introduction of an additional factor into the estimation that corrects changes in the topographic phase within the evaluation window by the different slope estimates, or using an external digital elevation model (for example, SRTM). Methods for estimating the coherence from the phase slope interferogram and slope compensation based on the two-dimensional fast Fourier transform were proposed earlier [14, 15].

In the first of these methods, the coherence estimation is performed by the ratio

$$\hat{\gamma}_2 = \sqrt{\frac{\left|\sum \dot{w}_1(i,j)\cdot \overline{w}_2(i,j)\right|}{\sqrt{\sum\left|\dot{w}_1(i,j)\right|^2\cdot\sum\left|\dot{w}_2(i,j)\right|^2}}} \tag{2}$$

where $\dot{w}_{1,2}(i,j) = \dot{z}_{1,2}(i,j)\cdot\overline{z}_{1,2}(i-1,j-1)$. Then, in the second Fourier method, the calculation of interferogram spatial modulation frequencies is used, which can be found as

$$[\omega_i,\omega_j] = \underset{\substack{i\le i_0\pm N\\ j\le j_0\pm M}}{\arg\max}\left(\mathrm{F}^2\left\{\dot{z}_1(i,j)\cdot\overline{z}_2(i,j)\right\}\right) \tag{3}$$

where ω_i,ω_j are the spatial frequencies that are evaluated in the interferogram estimation window, after which the spatial frequency demodulation is performed using a multiplier $\exp\left[-\mathrm{i}(\omega_i / i + \omega_j / j)\right]$ and then the evaluation is based on a formula similar to (1):

$$\hat{\gamma}_3 = \frac{\left|\sum \dot{z}_1(i,j)\cdot\overline{z}_2(i,j)\cdot\exp[-\mathrm{i}(\omega_i / i + \omega_j / j)]\right|}{\sqrt{\sum\left|z_1(i,j)\right|^2\cdot\sum\left|z_2(i,j)\right|^2}} \tag{4}$$

To improve the computational efficiency, the height of the 2FFT spectrum peak [15] can be used as a coherence estimate instead of the correlation coefficient, which will be the maximum for the full signals' correlation and approximately equal to the average product of the images intensities in the absence of correlation:

$$\hat{\gamma}_4 \approx \frac{P - \sqrt{\sum|z_1(i,j)|^2 \cdot \sum|z_2(i,j)|^2}}{\sum|z_1(i,j)|^2 \cdot \sum|z_2(i,j)|^2 - \sqrt{\sum|z_1(i,j)|^2 \cdot \sum|z_2(i,j)|^2}} \quad (5)$$

where P is the peak height of the amplitude FFT spectrum. The estimate turns out to be especially computationally efficient if the intensities ($|z(i,j)| = 1$) are neglected and only the phase relations are taken into account, then

$$\hat{\gamma}'_4 \approx \frac{P - \sqrt{MN}}{MN - \sqrt{MN}}. \quad (6)$$

3. Experimental results

Coherence maps are widely used as an adaptive parameter of phase noise filters in the interferometric processing of the imaging radar data. The spectral adaptive filter (Goldstein filter with Baran modification [13]) is the most common among phase noise suppression filters for SAR data and it uses the two-dimensional FFT spectra *F(k,l)* calculated in local windows (or blocks), which are then weighed as follows:

$$\dot{I}^F(m,n) = \mathrm{F}^{-1}\left\{\left|\dot{F}(k,l)\right|^{\alpha\left(1-\overline{\hat{\gamma}(k_0,l_0)}\right)} \cdot \dot{F}(k,l)\right\}. \quad (7)$$

where $\overline{\hat{\gamma}(k_0,l_0)}$ is the average of coherence estimate within the block; α is the coefficient of coherence scaling. Different coherence estimates $\hat{\gamma}_i$ should give different suppression results, so, the best estimate will be the one that will provide the best accuracy of the interferometric phase after the spectral adaptive filtration.

The accuracy is estimated by the standard deviation criterion as follows:

$$\sigma[\varphi^*] = \sqrt{\frac{1}{M \times N - 1}\sum_i\left\{\arg\left[\frac{\exp\left(j\varphi_i^* - 2\pi j\Psi_{0i}\right)}{\exp\left(j\overline{\varphi^*} - 2\pi j\overline{\Psi_0}\right)}\right]\right\}^2}. \quad (8)$$

where φ_i^* are the values of phase of interferogram after non-coherent accumulation (multilooking) or after the suppression of the phase noise, Ψ_{0i} are the absolute phase reference obtained by converting the reference of altitudes according to the formula:

$$\Psi_{0i} = 2\pi\left[h_{0i} / h_A\right]. \quad (9)$$

where h_A is the ambiguity height.

Comparative analysis of methods for the coherence maps calculation by formulas (1), (2), (4), (6) was carried out on experimental ALOS PALSAR radar interferometric data (the signal carrier frequency is 1,27 GHz, radiometric resolution is 5 bits), represented by an interferometric pair of images for a polygon containing different types of surface (fields, forests, urban and mining areas). The sample data were obtained in dual polarization mode (FBD), and the HH-polarization was used. The interferometric phase has an ambiguity height of 17.2 m (at the near edge of the scene); the spatial sampling interval was 15,0×3,1 m, and the scene size was 8000×1800 elements.

The reference data were represented by a set of 920 height ground control points (GCPs) with a vertical accuracy of 0.2 m, which covered an area of 1083 sq. km. The GCPs coordinates have been transformed into the WGS-84 coordinate system, and then reprojected the radar flight coordinate system of «slant range – azimuth» [14]. The influence of the coherence estimation window size on the accuracy of the interferometric phase after phase noise suppression by criterion (8) for different block sizes of the spectral adaptive filter (Goldstein filter with Baran modification) was analyzed.

The results are presented in figure 4, from which it can be seen that the use of coherence maps in the suppression of phase noise in many cases leads to a filtration accuracy improvement, which is expressed in a decrease in the relative phase standard deviation (STD) by a value about of 5%; but with the increase of the evaluation window size the benefit is reduced. The estimates (1), (4) and (6) behave themselves broadly similar, apart from the phase slope coherence (2), which gives the worst results for small filter block sizes (11×11) and the best results for medium sizes (21×21 ... 31×31; a benefit is more than 7% for a filter with a block size of 31×31).

4. Conclusion

The problem of the coherence estimation bias under the influence of the topographic phase slope (phase ramp) in interferometric data processing (InSAR) is investigated, and 3 ways to reduce the slope influence on the value of the estimate are considered. The paper presents a comparative analysis of the efficiency of four coherence estimates used in the SAR interferograms phase noise suppression by a spectral adaptive filter. It is shown that the application of coherence maps can improve the accuracy of the phase noise suppression results by 5..7%, and the best suppression is achieved by using the phase slope coherence estimation with relatively small window sizes.

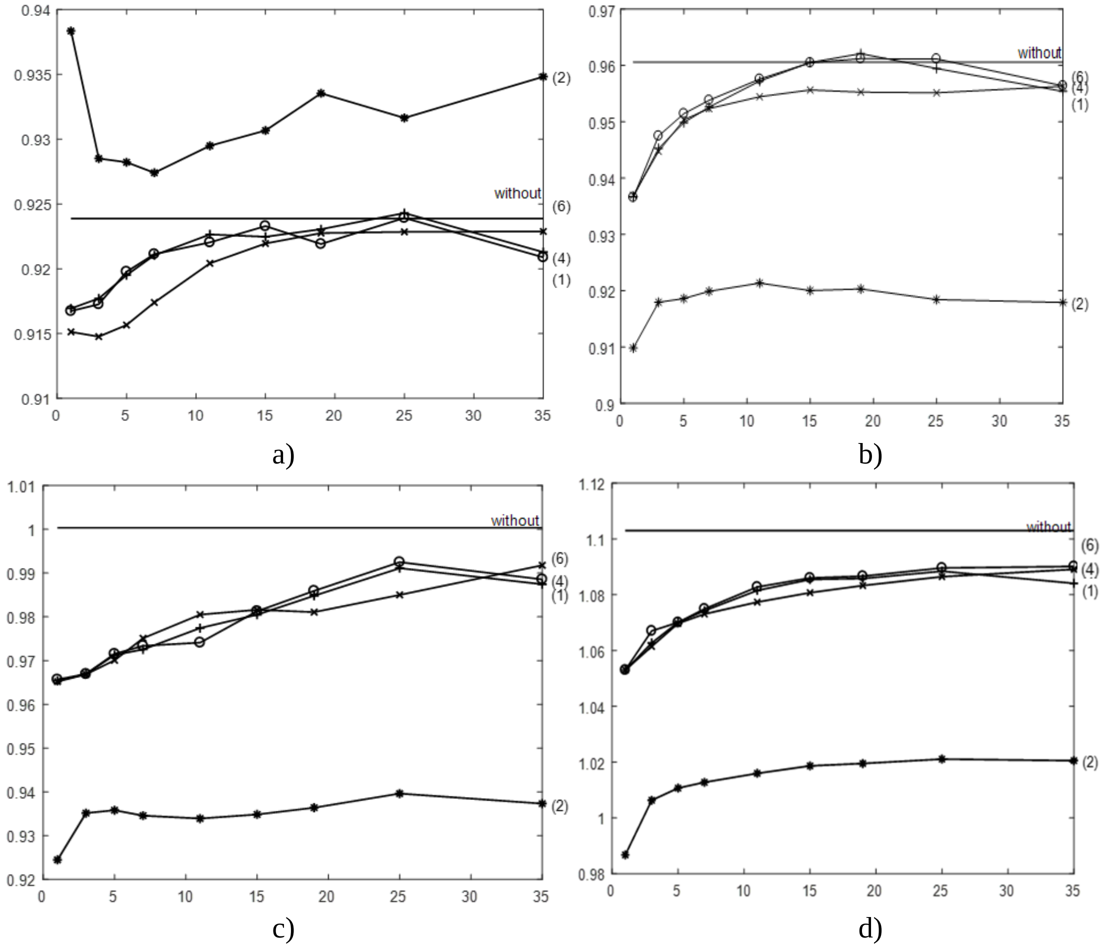

Figure 4. The dependence of the relative phase STD after the adaptive spectral filter (radians) from the coherence estimation window half-size N_0 ($N = M = 2N_0+1$): «*without*» (solid) is filtering without the use of coherence maps, *(1)* («+») is a classical estimation by formula (1), *(2)* («*») is the estimation of the coherence bias by the formula (2), *(4)* («o») is the estimate bias correction using 2FFT according to the formula (4), *(6)* («×») is the estimate based on the peak height of the 2FFT spectrum calculation by the formula (6). Cases: a) the size of the filtration block is 11×11, b) block size is 21×21 c) block size is 31×31, d) block size is 51×51.

5. References

[1] Monti Guarnieri A, Guccione P, Pasquali P and Desnos Y L 2003 Multi-mode ENVISAT ASAR interferometry: techniques and preliminary results *IEE Proc.-Radar Sonar Navig* **150(3)** 193-200

[2] Pavelyeva E A 2018 Image processing and analysis based on the use of phase information *Computer Optics* **42(6)** 1022-1034 DOI: 10.18287/2412-6179-2018-42-6-1022-1034

[3] Afanasyev A A, Zamyatin A V 2017 Hybrid methods for automatic landscape change detection in noisy data environment *Computer Optics* **41(3)** 431-440 DOI: 10.18287/2412-6179-2017-41-3-431-440

[4] Aduenko A A, Vasileisky A S, Karelov A I, Reyer I A, Rudakov K V and Strijov V V 2015 Algorithms of detection and registration of persistent scatterers in satellite radar images *Computer Optics* **39(4)** 622-630 DOI: 10.18287/0134-2452-2015-39-4-622-630

[5] Dorosinsky L G 2013 The research of the distributed objects' radar image recognition algorithms *23rd International Crimean Conference Microwave and Telecommunication Technology, Conference Proceedings* 1216-1217

[6] Abdelfattah R, Nicolas J M 2005 Coherence Estimation from Complex Coherence Map using Second Kind Statistics *Intern. Conf. on Image Processing* **II** 229-232

[7] Cattabeni M, Monti-Guarnieri A and Rocca F 1994 Estimation and Improvement of Coherence in SAR Interferograms *Geoscience and Remote Sensing Symposium* **4** 720-722

[8] Askne J, Hagberg J O 1993 Potential of interferometric SAR for classification; of land surfaces *Proc. Int. Geoscience and Remote Sensing Symp.* 985-987

[9] Gens R, Van Genderen J L 1996 SAR interferometry – Issues, techniques *Int. J. Remote Sens* **17** 1803-1835

[10] Lee H 2001 Analysis of Topographic Decorrelation in SAR Interferometry Using Ratio Coherence Imagery *IEEE Transactions on Geoscience and Remote Sensing* **39(2)** 223-232

[11] Touzi R, Lopes A and Vachon P W 1999 Coherence Estimation for SAR Imagery *IEEE transactions on geoscience and remote sensing* **37(1)** 135-149

[12] Lopez-Martinez C, Pottier E 2007 Coherence estimation in synthetic aperture radar data based on speckle noise modelling *Applied Optics* **46(4)** 544-558

[13] Baran I A, Stewart M P, Kampes B M, Persky Z and Lilli P 2003 Modification to the Goldstein Radar Interferogram Filter *IEEE Trans. Geosci. Rem. Sens* **41(9)** 2114-2118

[14] Sosnovsky A V, Kobernichenko V G 2016 *26th International conference "Microwave & telecommunication technologies"* 2716-2722

[15] Sosnovsky A V, Kobernichenko V G, Vinogradova N S and Tsogtbaatar O 2017 InSAR data coherence estimation using 2D fast Fourier transform *CEUR Workshop Proceedings* **1814** 98-105